ANTIOXIDANTS & REDOX SIGNALING
Volume 12, Number 12, 2010

DOI: 10.1089/ars.2009.2791

ORIGINAL RESEARCH COMMUNICATION

Glutaredoxin Regulates Apoptosis in Cardiomyocytes *via* NFκB Targets Bcl-2 and Bcl-xL: Implications for Cardiac Aging

Molly M. Gallogly,[1,*] Melissa D. Shelton,[1] Suparna Qanungo,[1] Harish V. Pai,[1] David W. Starke,[1] Charles L. Hoppel,[1] Edward J. Lesnefsky,[2,3] and John J. Mieyal[1,2]

Abstract

Cardiomyocyte apoptosis is a well-established contributor to irreversible injury following myocardial infarction (MI). Increased cardiomyocyte apoptosis is associated also with aging in animal models, exacerbated by MI; however, mechanisms for this increased sensitivity to oxidative stress are unknown. Protein mixed-disulfide formation with glutathione (protein glutathionylation) is known to change the function of intermediates that regulate apoptosis. Since glutaredoxin (Grx) specifically catalyzes protein deglutathionylation, we examined its status with aging and its influence on regulation of apoptosis. Grx1 content and activity are decreased by ~40% in elderly (24-mo) Fischer 344 rat hearts compared to adult (6-mo) controls. A similar extent of Grx1 knockdown in H9c2 cardiomyocytes led to increased apoptosis, decreased NFκB-dependent transcriptional activity, and decreased production (mRNA and protein) of anti-apoptotic NFκB target genes, Bcl-2 and Bcl-xL. Knockdown of Bcl-2 and/or Bcl-xL in wild-type H9c2 cells to the same extent (~50%) as observed in Grx1-knockdown cells increased baseline apoptosis; and knockdown of Bcl-xL, but not Bcl-2, also increased *oxidant-induced* apoptosis analogous to Grx1-knockdown cells. Natural Grx1-deficient cardiomyocytes isolated from elderly rats also displayed diminished NFκB activity and Bcl-xL content. Taken together, these data indicate diminution of Grx1 in elderly animals contributes to increased apoptotic susceptibility *via* regulation of NFκB function. *Antioxid. Redox Signal.* 12, 1339–1353.

Introduction

Cardiomyocyte apoptosis contributes significantly to loss of cardiac function following myocardial infarction (MI), as well as during the development of heart failure, and represents an important therapeutic target in cardiovascular medicine (reviewed in (23, 28, 57)). Cardiomyocytes from elderly animals exhibit increased apoptotic susceptibility, both at baseline and following oxidative injury (19, 26, 34). This increased apoptotic susceptibility may explain the increased risk of heart failure in elderly patients (20) and increased post-MI morbidity and mortality in human patients and animal models (24, 52, 55). Therefore, it is important to characterize molecular mechanisms that contribute to increased apoptosis in aging cardiomyocytes as a prelude to developing therapeutic strategies to minimize cardiac injury in the elderly population. This work examines the role of diminution of glutaredoxin in cardiomyocytes as a basis for increased susceptibility of cardiomyocytes of the elderly to oxidant-induced apoptosis. At the outset of this study it was our hypothesis that perturbation of redox homeostasis associated with diminution of glutaredoxin activity predisposes cardiomyocytes of elderly animals to greater oxidant injury. This working hypothesis is consistent with the work of Rebrin *et al.* (40) who reported a pro-oxidizing shift in thiol–disulfide balance in mice and *Drosophila* with aging.

Human glutaredoxin (Grx1) has been characterized as a thiol–disulfide oxidoreductase enzyme that specifically and efficiently catalyzes protein deglutathionylation (10). Protein S-glutathionylation is a reversible post-translational modification involving mixed disulfide formation between a protein cysteine and glutathione (GSH), and it serves both as

[1]Department of Pharmacology, Case Western Reserve University, School of Medicine, Cleveland, Ohio.
[2]Department of Internal Medicine, Division of Cardiology, Virginia Commonwealth University, and Medical Service, McGuire Veterans Affairs Medical Center, Richmond, Virginia.
[3]Department of Medicine, Division of Cardiology, Case Western Reserve University and Medical Service, Veterans Affairs Medical Center, Cleveland, Ohio.
*Studies completed in partial fulfillment of the requirements for the Ph.D. degree, Case Western Reserve University.

protection against irreversible oxidation and as a mechanism of redox signal transduction (reviewed in Ref. 30). Protein glutathionylation is generally triggered by oxidative stimuli (*e.g.*, growth factor treatment (53), H_2O_2 exposure (7), ischemia-reperfusion (8)), but also represents the basal status of certain protein cysteines in resting cells (*e.g.*, actin (53), mitochondrial Complex II (6), pro-caspase-3 (36), and IκB kinase (41)).

Knowledge is growing about the role of Grx1 as a regulator of apoptosis in mammalian cells, including cardiomyocytes. The extent of cardiomyocyte apoptosis was increased in Grx1-knockout mice after ischemic challenge and decreased in mice overexpressing Grx1 (27). The activities of several mediators of apoptosis have been reported to be modulated by reversible glutathionylation under the control of GRx1 (*e.g.*, procaspase-3 (36), p65 (39), IKK (41)). Overexpression of Grx1 in H9c2 cardiomyocytes was cytoprotective, diminishing H_2O_2-induced apoptosis likely *via* redox regulation of Akt (32). Likewise increased expression of Grx1 in HEK cells was protective, increasing survival after glucose deprivation *via* Grx1 complex formation with ASK1 (48). In certain cases, Grx1 has been reported to enhance apoptosis; for example, Grx1-catalyzed deglutathionylation (activation) of procaspase-3 enhances apoptosis in endothelial cells exposed to TNFα and actinomycin D (36). Thus, the effect of Grx1 on apoptotic susceptibility seems to be cell type- and stimulus-dependent, likely reflecting distinct targets of regulation by Grx1 in each case.

NFκB is recognized as an important regulator of cell fate in normal and diseased myocardium (reviewed in Ref. 18), and it has been implicated in the cardioprotective effects of preconditioning (29) and TNF-α stimulation (2, 33). Multiple members of the NFκB signaling pathway (*e.g.*, Akt, IKK, p65, and ubiquitin ligase (reviewed in Ref. 46) are reported to be inhibited by S-glutathionylation, and thus represent potential targets for regulation by Grx. Indeed, alterations in Grx activity have been linked to changes in NFκB activity in rodent airway (41), rat retinal glial (45), and human kidney (14) cell lines.

Here, we report an age-associated diminution of Grx1 in Fischer 344 (F344) rat heart, an observation which prompted mechanistic studies in H9c2 cells to explore the potential contribution(s) of decreased Grx1 to cardiomyocyte apoptosis in the elderly. We found that diminution of Grx1 in H9c2 cardiomyocytes sensitized them to apoptosis, both at baseline and following oxidative stress, likely *via* decreased activity of NFκB and subsequent decreased expression of target genes Bcl-2 and Bcl-xL. NFκB-dependent transcription and Bcl-xL content were also decreased in the aging F344 rat heart, suggesting that decreased Grx1 contributes to age-associated increases in cardiomyocyte apoptosis *via* an analogous mechanism.

Materials and Methods

General materials

Unless otherwise specified, cell culture media, serum, and antibiotics were purchased from Invitrogen (Carlsbad, CA), and reagent grade chemicals were obtained from Sigma (St. Louis, MO).

Animals

Adult (6-mo) and elderly (24-mo) male Fisher 344 rats were obtained from National Institute on Aging colonies (Harlan, Indianapolis, IN; Taconic, Germantown, NY) and housed in the animal facilities of the Louis Stokes Veterans Affairs Cleveland Medical Center and Case Western Reserve University. Animals were acclimated for at least 1 week before use, and used for experiments within 4 months. The Animal Care and Use Committees of Case Western Reserve University and the Louis Stokes Veterans Affairs Cleveland Medical Center approved all animal protocols.

Culture and maintenance of H9c2 cells

H9c2 cells (rat embryonic cardiomyocytes) (gift from Laura Nagy, Cleveland Clinic Foundation) were cultured in DMEM (Invitrogen #11965-092) with 10% certified fetal bovine serum (FBS) and 1X "antibiotic/antimycotic" (1 U/ml penicillin, 1 μg/ml streptomycin, and 0.025 ng/ml amphotericin-B) at 37°C, 5% CO_2. Cells were passaged after reaching confluence. All experiments utilized cells of passage number 10–30.

Knockdown of Grx1, Bcl-2, and Bcl-xL

H9c2 cells were plated at a density of $2–3\times10^4$ per well in 6-well culture dishes, then incubated overnight. The cells were then rinsed twice with serum-free medium and transfected with control (nontargeting) or Grx1-, Bcl-2-, or Bcl-xL-targeted siRNA (25–100 n*M*, Thermo Scientific, Waltham, MA) with oligofectamine (3 μl/well, Invitrogen) according to the manufacturer's instructions. Four h later, 50 μl DMEM containing 30% serum (no antibiotics) was added to each well. Cells were analyzed for protein content and/or susceptibility to apoptosis 24–48 h later. For each siRNA target, extent of knockdown was titrated by varying the dose of siRNA and determining the percentage of knockdown by Western blot analysis (see below) for 3 days post-transfection.

Stable knockdown of Grx1

The following DNA sequences were subcloned individually into the p.SUPER.retro.puro vector (Oligoengine, Seattle, WA) using T4 DNA ligase: 1) 19 random residues corresponding to no known gene in the rat or mouse genome; 2) base pairs 94–112 of the rat Grx1 gene; 3) rat Grx1 base pairs 231–249; or 4) rat Grx1 base pairs 300–318. For transfection, 6 μg of Grx1-coding plasmid DNA (2 μg of each construct, for knockdown cells) or 2 μg of plasmid containing the scrambled sequence (for control cells) was used to transfect 6 million BOSC cells (gift of Dr. George Stark, Cleveland Clinic Foundation) plated on a 100 mm dish in serum-free DMEM using Lipofectamine and PLUS reagents (Invitrogen), according to the manufacturer's instructions. After incubation for 4 h at 37°C, 5% CO_2, medium was removed by aspiration and replaced with DMEM containing 10% heat-inactivated FBS and 1X antibiotic/antimycotic. After 24 h (day 2), medium was collected from BOSC cells and diluted 1:1 with DMEM (10% FBS, 1X antibiotic/antimycotic). After addition of polybrene (5-dimethyl-1,5-diazaundecamethylene polymethobromide, hexadimethrine bromide) (10 μg/ml final concentration), the mixture was sterile-filtered and added to 100,000 H9c2 cells plated on a 100 m*M* dish. Fresh medium was added to the BOSC cells, and this procedure was repeated on days 3 and 4. On day 5, 2 μg/ml puromycin (Sigma) was added to the H9c2 cell medium. Cells were selected for approximately

7 days, then analyzed for Grx1 content and total Grx activity. Grx knockdown was maintained for weeks in the presence of puromycin and H9c2 cells up to 6 passages post-transfection were used for experiments.

Determination of Grx activity

For measurement of Grx activity in F344 rat heart tissue, rat myocardium (250 mg) from adult (6–10-mo) or elderly (24–28-mo) F344 rats was homogenized at 4°C in 1 ml buffer containing potassium phosphate (10 m*M*), pH 7.5; EDTA (5 m*M*); phenylmethane-sulfonyl fluoride (50 μM); and 2 m*M* β-mercaptoethanol using a glass homogenizer. The homogenate was centrifuged at 4 °C sequentially at 700, 2000, and 10,000 *g* for 10 min each. Supernatants were dialyzed overnight at 4°C against the same buffer at a ratio of 1 ml supernatant: 1000 ml dialysis buffer (with two changes of buffer) to remove GSH. Grx activity was measured by the radiolabel assay, as described by Chrestensen *et al.* (7).

For cardiomyocytes isolated from F344 rats (see below), cell pellets were homogenized in NP-40 lysis buffer (50 m*M* Tris-HCl, pH 8, 150 m*M* NaCl, 1% NP-40) in disposable, hand-held homogenizers (Fisher, Fairlawn, NJ) and cleared by centrifugation at 10,000×*g* for 5 min at 4°C, then Grx activity was measured spectrophotometrically as described in (17). Activity was normalized to protein content measured by the BCA assay (Pierce, Fairlawn, NJ).

Grx activity in H9c2 cells was measured spectrophotometrically, following trypsinization of control and Grx1 knock-down cells, lysis in NP-40 lysis buffer on ice for 10 min, and clearing of lysates by centrifugation at 10,000 *g* (4°C). Supernatants (5–20 μl) were analyzed for Grx activity and for protein content as described above. For all analyses, Grx activity was determined within the linear range of concentration dependence of activity on volume (μl) of lysate added.

Western blot analysis

H9c2 cells were lysed in NP-40 lysis buffer containing Sigma Protease Inhibitor Cocktail (5%, final). The cytosolic fraction of F344 rat heart homogenate was prepared as described above for analysis of Grx activity. Lysates/homogenates containing 10–100 μg of protein were incubated with 4X sample buffer (100 ml 0.5 *M* Tris-HCl, pH 6.8, 80 ml glycerol, 160 ml 10% SDS, 20 ml 1% bromophenol blue) and DTT (10 m*M*, final) for 10 min at 95°C; then, IAM (25 m*M*, final) was added and samples were heated at 95°C again for 5 min. Samples were resolved on 12.5% polyacrylamide gels and transferred to PVDF membranes. Membranes were blocked with nonfat milk (5% in Tris-buffered saline, TBS) for 1 h at room temperature, then with primary antibody in 5% milk/TBS overnight at 4°C. Membranes were washed with TBS (3×10 min), then incubated with the appropriate secondary antibody (1:10,000) in 5% milk/TBS for 1 h and washed again. ECL or Pico Supersignal developing reagent (Pierce) was used for chemiluminescent detection of antibody binding. Primary antibodies were anti-Grx1 ((45), 1:1000), anti-actin (Sigma, clone AC-74, 1:60,000), anti-GAPDH (Calbiochem, Gibbstown, NJ, 1:100,000), anti-Bcl-2 (BD Biosciences, San Diego, CA, 1:500), anti-Bcl-xL (Cell Signaling Technologies, Danvers, MA, 1:5000), anti-p50 (Santa Cruz, Santa Cruz, CA, sc-114, 1:1000), anti-p65 (Santa Cruz, sc-372, 1:2000). Secondary antibodies were anti-rabbit or anti-mouse (both from Jackson Laboratories, Bar Harbor, ME). *For detection of Bcl-2 and Bcl-xL, 0.1% Tween (final) was added to the TBS to minimize background signal.*

Determination of Trx1 content and activity

Heart apices from F344 rats were quick-frozen in liquid N_2, then thawed and homogenized for 20 s in homogenization buffer (20 m*M* Tris, pH 7.5, 1% Triton X-100, 100 m*M* NaCl, 40 m*M* NaF, 1 m*M* EDTA, 1 m*M* EGTA, 5% Sigma Protease Inhibitor Cocktail) using a Polytron homogenizer (Brinkmann, Delran, NJ) set at 70% maximum speed. Homogenates were incubated on ice for 30 min, then centrifuged at 10,000 *g* for 10 min. Protein content of supernatants was determined by the BCA assay (Pierce) and Trx1 content was analyzed by Western blot analysis (see above). (The polyclonal sheep, anti-human Trx1 antibody (Quality Controlled Biochemicals, Hopkinton, MA) was generated from peptide sequences of the Trx1 protein, and used at a dilution of 5 μg/ml).

Trx activity in heart tissue homogenates was measured according to reduction of insulin disulfides in the presence of excess exogenous TR and NADPH and detected with DTNB, as described in Arner *et al.* (1). Separate experiments documented linear time- and homogenate concentration-dependence under the assay conditions. Thus, 60 μg of heart homogenate (protein content) was incubated in a final volume of 65 μl containing 0.3 m*M* insulin, 0.66 m*M* NADPH, 2.5 m*M* EDTA, and 38 mU TR (shown to be nonlimiting) in 85 m*M* HEPES, pH 7.6, for 40 min at 37°C. The reaction was stopped by addition of 200 μl of 8 *M* guanidine-HCl solution containing 1 m*M* DTNB, and absorbance at 405 nm was read immediately in the plate reader. Background absorbance, likely due to thiols and released heme in the denatured homogenate, was subtracted and the net change in A_{405nm} at 40 min was converted to specific enzyme activity (nmol thiol/min/mg) according to a standard curve for thiol (GSH) content generated under the same conditions.

Determination of corresponding reductase activities

Heart tissue homogenates were prepared as decribed above, and TR and GR activities were measured as described by Starke *et al.* (49).

Real-time PCR

Cells transfected with control or Grx1 siRNA for 48 h were collected in a total volume of 1 ml Trizol (Invitrogen) per 6 wells of a 6-well culture dish, and RNA was isolated from each sample using the RNeasy kit (Qiagen, Valencia, CA). To determine relative quantities of Bcl-2 mRNA, cDNA was generated from each sample according to the ABI High Capacity RT kit protocol (200 ng RNA input), and real-time PCR was performed on an Applied Biosystems 7500 Fast Real Time PCR system according to the manufacturer's protocol, using primers for 18S rRNA or rat Bcl-2 (Applied Biosystems, Foster City, CA). To confirm the diminution of Bcl-2 mRNA and to determine the effect of Grx1 knockdown on Bcl-xL mRNA content, relative quantities of Bcl-2 and Bcl-xL mRNA were determined simultaneously using a PCR-array from SA

Biosciences (Frederick, MD). cDNA from control and Grx1 knockdown cells was generated from Trizol lysates using the SA Biosciences RT^2 First Strand Kit (500 ng input), and samples were loaded onto a 384-well plate containing probes for 84 apoptosis-related genes and 6 housekeeping genes (Cat. No. PARN-012, SA Biosciences). PCR analysis was performed on an ABI 7900 Real-Time PCR system (Applied Biosystems) using SYBR Green/ROX Master Mix (Cat. No. PA-012-8, SA Biosciences). Cycle conditions were: (a) hold at 95°C for 10 min; (b) 40 cycles of 15 s at 95°C, followed by 1 min at 60°C. Relative changes in gene expression were calculated using the $\Delta\Delta C_t$ method. GAPDH was used to normalize the calculated relative quantities of mRNA. Duplicates of each sample were averaged prior to normalization and calculation of relative expression. A total of three pairs of samples were analyzed, and Grx1 knockdown was confirmed separately for each set of samples by Western blot analysis.

H_2O_2 treatment of H9c2

H9c2 cells were incubated in culture medium with or without H_2O_2 (Fisher Scientific, 400 μM final) for 5 min at 30°C/5% CO_2. Following treatment, medium on all cells was replaced with fresh medium without H_2O_2. For wild-type H9c2 cells, treatments were performed in medium containing 10% serum and 1X antibiotic/antimycotic (normal culture medium). For H9c2 cells transfected with siRNA, treatment was done in medium containing 1.4% serum (the final serum concentration following transfection) without antibiotic/antimycotic. H_2O_2 dose-response experiments on wild-type cells showed no difference in apoptosis in wild-type cells treated with H_2O_2 in 1.4%- *vs*. 10%-serum medium (data not shown). 24 h after treatment, cells were analyzed for apoptosis by Hoechst staining (see below).

Simulated ischemia/reperfusion of H9c2 cells

H9c2 cells were incubated with glucose-free Krebs-Ringer-Henseleit (KRH) buffer (21). Cells at pH 6.2 were placed in a plexiglass chamber (Billups-Rottenberg, Del Mar, CA) which was made hypoxic by sparging with 95% N_2, 5% CO_2, 0.5% O_2 for 4 min at 2.5 psi. The chamber was placed in the same incubator as the one containing the cells at pH 7.4 (normoxic condition), and all cells were incubated for 3 h. Hypoxic H9c2 cells were then removed from the chamber and the medium on all cells was replaced with KRH buffer, pH 7.4. Cells were incubated for 2 h more to simulate reperfusion, then analyzed for apoptosis by Hoechst staining (*see below*).

Determination of apoptosis

H9c2 cells were incubated with Hoescht 33342 dye (Invitrogen, H1399, 1 μg/ml final) for 10 min and nuclear condensation and fragmentation were visualized with a Leica fluorescence microscope equipped with a DAPI filter. The percentage of apoptotic cells was calculated by dividing the number of cells with condensed and/or fragmented nuclei by the total number of cells counted in each well of a 6-well plate. At least 300 cells/well were counted, and each well represented one determination of a triplicate experiment. All cell counting was performed in a blinded fashion.

NFκB activity in H9c2 cells

24 h after transfection with siRNA (control or Grx1), H9c2 cells were co-transfected for 12 h with 1 μg of 5X-NFκB Luciferase plasmid (Stratagene, La Jolla, CA) and 0.1 μg of Renilla plasmid (Promega, Madison, WI) according to the Lipofectamine (Invitrogen) reagent protocol. 24 h later, luciferase activity was assayed using the Dual-Luciferase assay system (Promega) by measuring emission with a luminometer (SOFTmax PRO software, Molecular Devices, Sunnyvale, CA). NFκB activity is expressed as the ratio of firefly luciferase-dependent luminescence to Renilla luciferase-dependent luminescence.

Effect of NFκB inhibition on apoptotic susceptibility

25,000 H9c2 cells were seeded on each well of a 6-well dish in regular medium *without antibiotics* and cultured for 24 h. Cells were co-transfected with 1 μg/well NFκB-luciferase plasmid (Stratagene) and 0.1 μg/well Renilla plasmid (Promega) using Lipofectamine 2000 (Invitrogen) at a ratio of 1 μg DNA:2 μL Lipofectamine 2000. Approximately 8 h after the start of transfection, medium was replaced with antibiotic-free culture medium containing BMS 345541 (4(2-aminoethyl)amino-1,8-dimethylimidazo(1,2-a)quinoxaline) (0–20 μM) and cells were cultured overnight. The next morning (24 h after transfection, ~14 h after BMS treatment), cells were either collected for determination of NFκB activity (Luciferase assay, see above) or assayed for apoptotic susceptibility. Specifically, half of the cells were treated with H_2O_2 (see above) and half were subjected only to a change of medium. After 24 h, apoptosis was assessed by Hoechst staining (see above). *Note: For BMS-treated cells, Firefly-luciferase activity was normalized to protein content (A_{280nm}) rather than Renilla-luciferase activity because BMS treatment appeared to interfere with measurement of Renilla activity.*

Isolation of primary cardiomyocytes

Adult and elderly F344 rats were heparinized (3,000 units IP) 5 min prior to administration of pentobarbital (100 mg/kg). Cardiomyocytes were then isolated as described by Patel *et al.* (37), with modifications designed to maximize the yield of elderly myocytes. Specifically, hearts were perfused with ~400 U/ml Collagenase Type II (Worthington Biochemical, Lakewood, NJ), and following digestion, the ventricles were minced in 10 ml collagenase-free heart media in order to minimize damage to the fragile elderly myocytes.

Minced cardiac tissue triturated for 3 min with a disposable plastic pipettor and filtered through an 80 μm steel mesh screen. The filtrate volume was brought to 25 ml by addition of ~15 ml wash buffer (heart media containing 1% BSA and 20 μM $CaCl_2$), then centrifuged at low speed (~170 *g*) for 25 s. 20 ml of the supernatant was then removed, 25 ml wash buffer was added to the loose pellet, and the tube was gently inverted 2–4 times. After 10 min settling at room temperature, the centrifugation and resuspension was repeated for a total of two washes. Ca^{2+} was reintroduced to cells in wash buffer by two stepwise additions (decreased from four additions to minimize myocyte manipulation) of 150 μl $CaCl_2$ solution (100 mM stock) to achieve a final Ca^{2+} concentration of 1.0 mM (reported to be better tolerated by cardiomyocytes

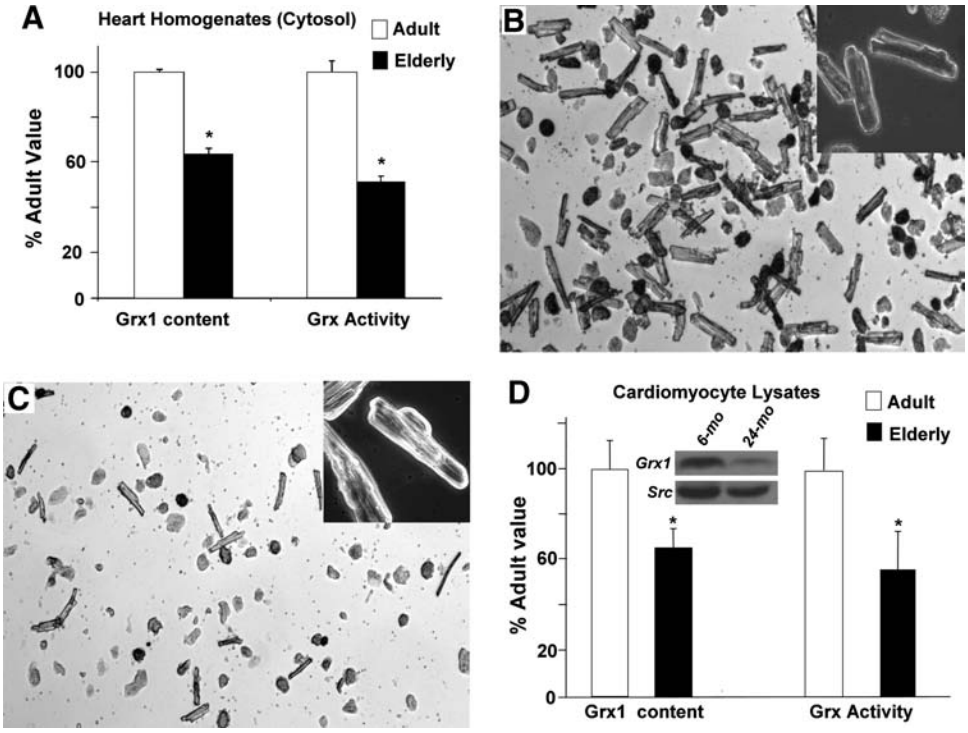

FIG. 1. Grx1 content and activity decrease with age in heart tissue cytosol and in isolated cardiomyocytes from F344 rats. (**A**) Grx1 content in cytosolic fractions of heart tissue homogenates from adult (6–10 mo) and elderly (24–28 mo) F344 rats was determined by semiquantitative Western blot analysis with anti-Grx1 antibody. Band densities from cytosolic samples were converted to amounts of Grx1 protein by comparison to known amounts of purified Grx1 protein analyzed on the same blot, within the linear range of concentration dependence. Grx1 content in elderly rat hearts (1.1 ± 0.04 pmol Grx1/mg protein) was normalized to content in 6-mo animals (1.7 ± 0.02 pmol Grx1/mg protein). Total Grx activity was determined by monitoring GSH-dependent release of radiolabel from [^{35}S] BSA-SSG as described in *Materials and Methods* and in Ref. (7). Activity in elderly hearts (mean ± SEM = 0.94 ± 0.02 nmol [^{35}S] GSSG released/min/mg protein) was normalized to the activity observed in adult hearts (mean ± SEM = 1.67 ± 0.1 nmol [^{35}S] GSSG released/min/mg). *Open bars*, adult; *closed bars*, elderly. *$p < 0.001$ *vs*. adult ($n = 3$ for each age). (**B–C**) Representative microscopy images of cardiomyocytes isolated from adult (**B**) and elderly (**C**) F344 rat hearts. Myocytes were isolated as described in *Materials and Methods*, allowed to adhere to laminin-coated dishes for 1 h, and visualized by phase contrast microscopy (10X magnification). *Inset*, 40X magnification showing characteristic striations on the rod-shaped cells. (**D**) Representative Western blot for Grx1 content is shown for analysis of two pools of six lysates of cardiomyocytes isolated from young adult (6-mo) and elderly (24-mo) Fischer 344 rats, respectively. Individual Western blots and densitometric analysis were performed on each of five independent samples of cardiomyocytes from each age group of rats (young adult and elderly). The *bar graph* on the left represents the means ± SEM (normalized to 100%) of these separate Western blot analyses. Quantification of Grx1 content (normalized to Src) shows a decrease to $65 \pm 8.9\%$ in cardiomyocytes from elderly rats (24-mo) as compared to young adult (6-mo) animals. *Open bars* (□), adult; *closed bars* (■), elderly. *$p = 0.03$ *vs*. adult ($n = 5$).

The *bar graph on the right* illustrates total Grx activity in cardiomyocytes isolated from young adult (6-mo) and elderly (24-mo) F344 rat hearts. Mean values ± SEM were normalized to the value from 6-mo rats (42.5 ± 5.5 nmol NADPH oxidized (*i.e.*, GSSG produced)/min/mg total protein *vs*. 24.3 ± 6.8 nmol/min/mg for 24-mo rats). *$p < 0.01$ ($n = 3$–4).

from elderly rats (25)) than the typical concentration of 1.2 m*M* used for isolation of cardiomyocytes from neonatal or adult animals. After each addition of $CaCl_2$, cells were gently mixed and allowed to settle for ~10 min. After the second settling, the cell supernatant (wash buffer containing 1.0 m*M* Ca^{2+}) was replaced with plating medium (Medium 199 with Hank's salts, 4% FBS, 1% penicillin/streptomycin). Yields were typically ~$1–2 \times 10^6$ cells (~50% rods) from adult hearts, and $2.5–5 \times 10^5$ cells (10%–30% rods) from elderly hearts. Comparison of Grx activity in adult and elderly myocytes indicated that the myocyte preparations exhibit the same age-associated decline in Grx activity observed in heart tissue (see Results), indicating that representative populations of cardiomyocytes were isolated from rats of each age group.

Determination of NFκB activity in primary cardiomyocytes

Following isolation, cardiomyocytes in plating medium (Medium 199 containing Hank's salts, FBS (4%), and penicillin/streptomycin (1%)) were allowed to settle by gravity, then resuspended and divided into 3–6 (for elderly rats) or 12–24 (for adult rats) equivalent volumes, according to the estimated yield (*i.e.*, amount of settled cells). Each sample was pelleted by centrifugation at ~175 *g* for 10–20 s, supernatants

(containing medium and fibroblasts) were removed by aspiration, and each pellet was resuspended in 200 μl maintenance medium (4 parts Medium 199 with Hank's salts, BSA (1%) and penicillin-streptomycin (1%); 1 part Joklik Modified Medium (Sigma)) containing Renilla (MOI = ~20) and NFκB-Luciferase (MOI = ~100) or MCS (negative control, MOI = ~100) adenovirus (Vector Biolabs, Philadelphia, PA) and incubated at 30°C/5% CO_2 for 1 h. Following incubation, each mixture of cardiomyocytes in virus-containing medium was diluted into 2 ml maintenance medium and added to one well of a 6-well tissue culture plate pre-coated with mouse laminin (Invitrogen). For elderly rats, cardiomyocytes from two hearts were plated sequentially onto the same 3–6 wells in order to achieve comparable cell density and to ensure sufficient yield for the Luciferase assay. Cardiomyocytes were cultured for 24 h, then collected in 150 μl 1X Passive Lysis Buffer (Promega) according to the manufacturer's protocol. Twenty μl of each sample were used to determine Luciferase and Renilla activities using the Dual-Luciferase assay system (Promega), as described above. For each preparation of myocytes, at least three replicate determinations were performed and then averaged to represent a single experiment (*i.e.*, n number). Cells infected with MCS adenovirus exhibited no Luciferase activity above background (*i.e.*, Luciferase and Stop & Glow reagents alone, data not shown).

Statistical analysis

Unless otherwise indicated, data are reported as mean ± standard error (mean ± SEM). On occasion, individual data points more than two standard deviations from the mean were considered to be outliers and omitted. Differences between data sets were tested for statistical significance using Student's *t*-test (Microsoft Excel) on primary data.

Results

Grx1 content and total Grx activity are decreased in the hearts of elderly F344 rats

Cytosolic fractions of heart tissue from adult (6–10 mo) and elderly (24–28 mo) F344 rats were analyzed by semiquantitative Western blotting and revealed an age-associated decrease in Grx1 content of approximately 40% (Fig. 1A, left). Total Grx activity (*i.e.*, GSH-dependent deglutathionylation of protein-SSG substrate) was diminished by a similar margin in the elderly (Fig. 1A, right). This decrease in Grx activity was not due to a change in the GSSG reductase (GR) coupling enzyme. Thus, GR activity showed a trend toward an increase in the elderly, but this was not statistically significant (8.9 ± 1.9 nmol/min/mg (adult) *vs.* 12 ± 1.9 (elderly); $n = 6$, $p = 0.29$).

In contrast to the distinct loss in Grx content and activity, similar changes were *not* observed for thioredoxin 1 (Trx1) content and activity, nor for thioredoxin reductase (TR) activity (Fig. 2). Trx1 contents (6-mo *vs.* 24-mo) were indistinguishable by Western blot and densitometric analysis compared to Trx1 standards and loading controls, measured both in heart homogenates and in isolated cardiomyocytes (Fig. 2, panel A). Thioredoxin activity tended toward a modest decrease in the elderly (Fig. 2, panel B left), but the apparent difference was not statistically significant ($p = 0.44$, $n = 4$); and thioredoxin reductase (TR1) activity clearly was unchanged (Fig. 2, panel B right). Based on these data, we focused our further studies on the impact of diminution in Grx activity and content.

To confirm that the age-associated diminution of Grx1 occurs in *cardiomyocytes* (which contribute the majority of cardiac protein to heart tissue), cardiac myocytes were isolated from adult and elderly F344 rats *via* adaptation of the method of Patel *et al.* (37). Although preparations from elderly animals yielded fewer cells than those from adult animals (0.3–0.5×10^6 cells for elderly *vs.* 1–2×10^6 cells from adults), both preparations after plating on laminin and changing the medium yielded mostly adherent rod-shaped cardiomyocytes with similar overall morphology (Figs. 1B and 1C). Analysis of lysates from isolated cardiomyocytes (Fig. 1D) indicated a similar diminution in Grx1 content and Grx activity as observed in heart tissue homogenates and cytosol preparation (Fig. 1A).

Knockdown of Grx1 in H9c2 cells

To investigate the specific contribution(s) of decreased Grx1 to increased apoptotic susceptibility in cardiomyocytes, independent of other changes that may occur upon aging, Grx1 was knocked-down selectively using siRNA in H9c2 cells (rat embryonic cardiomyocytes). siRNA dose and post-incubation time were adjusted to achieve a diminution of Grx1 in H9c2 cells that was similar to the decrease observed in aging cardiomyocytes (Fig. 3A). Thus, in H9c2 cells transfected with Grx1-targeted siRNA, Trx1 content was not affected as expected, and Grx1 content and activity (Figs. 3A and 3B) were decreased by approximately 50% compared to wild-type and to control cells (transfected with a pool of nontargeted siRNA). A comparable diminution of Grx1 content and activity was achieved when Grx1 was knocked-down stably using shRNA (*i.e.*, Grx1 content in shRNA knockdown cells was 31 ± 16% lower than in cells infected with scrambled (control) shRNA; total Grx activity was diminished by 40 ± 5% in shRNA knockdown cells compared to control cells).

Grx1 knockdown increases oxidant-induced apoptosis in H9c2 cells

To test the potential contribution of diminished Grx1 on susceptibility to apoptosis following an oxidative insult, control and Grx1-deficient H9c2 cells were subjected to simulated ischemia reperfusion (sIR) (21), or treated with H_2O_2, previously shown to trigger a classical apoptotic cascade in H9c2 cells (13). Following treatment, apoptosis was assessed by Hoechst staining. Grx1-deficient cells exhibited increased apoptosis compared to control cells, both at baseline and following oxidative stress; that is, the percentage of apoptotic cells was approximately doubled in Grx1-deficient cells compared to control cells following simulated IR or H_2O_2 treatment (Fig. 4A). Analogous results were observed in H9c2 cells with stable knockdown of Grx1 (Fig. 4B).

NFκB transcriptional activity is decreased in Grx1-deficient cells

We hypothesized that decreased activity of the NFκB pathway contributes to the increased apoptotic susceptibility of Grx1-deficient cells. To determine whether Grx1 knockdown results in decreased transcriptional activity of NFκB, NFκB-dependent transcription was measured in control and

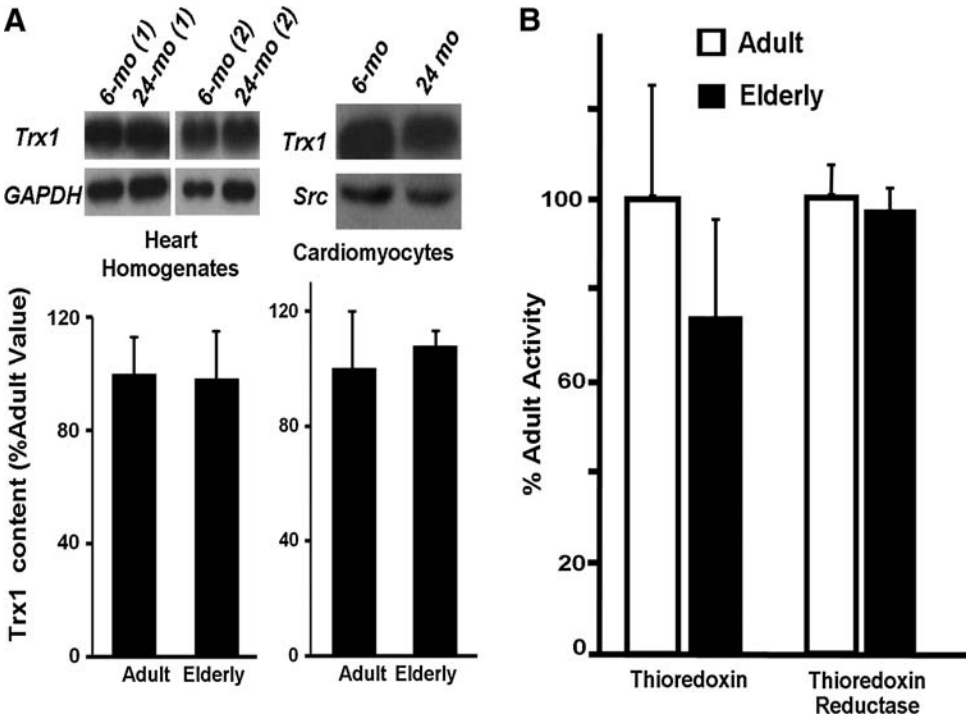

FIG. 2. Trx1 content, and Trx and TR activities show little if any change with age in heart homogenates and in isolated myocytes from F344 rats. (**A**) (*Left panel*) Western blot analysis was performed using anti-Trx1 antibody in heart homogenates from adult (6-mo) and elderly (24-mo) F344 rats. Representative Western blots from two sets of rat homogenates for each age group (6-mo (1), (2) and 24-mo(1), (2)) are shown. Trx1 content is normalized to GAPDH (loading control) and the *bar graph* is expressed as a ratio of the relative quantities of Trx1 in the heart homogenates from elderly rats as compared to adult rats. Data represent mean ± SEM ($n = 11$ for 6-mo and $n = 13$ for 24-mo). (*Right panel)* Representative Western blot showing unchanged Trx1 content in a pool of six lysates each of cardiomyocytes isolated from young adult (6-mo) and elderly (24-mo) Fischer 344 rats. The *bar graph* represents the mean Trx1/Src ratio (normalized to 100%) of two separate Western blot analyses of three different sets of pooled lysates corresponding to cardiomyocytes isolated from young adult and elderly rats. One type of pool was made from three individual preparations of cardiomyocytes of each age group, lysed separately in RIPA buffer, frozen at −80°C, then thawed and combined for analysis. The second type of pool of three different individual cardiomyocyte preparations were lysed in NP-40 buffer and processed analogously. The third type of pool contained equal portions of pool type 1 and pool type 2 for each age group. Although the data represent a composite contributed by six individual biological samples of each age group, they were analyzed as an "$n = 3$." (**B**) Total Trx and TR activities in homogenates isolated from 6-mo and 24-mo F344 rat hearts were determined as described in *Materials and Methods*. Activities in elderly hearts (mean ± SEM = 1.42 ± 0.39 nmol thiol/min/mg for Trx; 1.63 ± 0.08 μmol NADPH oxidized/min/ml for TR) were normalized to the corresponding activities observed in adult hearts (mean ± SEM = 1.85 ± 0.44 nmol thiol/min/mg total protein for Trx; 1.68 ± 0.13 μmol NADPH oxidized/min/ml for TR). *Open bars* (□), adult; *closed bars* (■), elderly. No significant differences (elderly *vs.* adult) were found for the Trx or TR activities; $n = 4$ for Trx, and $n = 3$ for TR.

Grx1-deficient cells using a standard dual-Luciferase reporter assay. Indeed, NFκB transcriptional activity was partially diminished (37 ± 11% decrease) in Grx1 knockdown cells compared to control cells (Fig. 5). This decrease is unlikely to reflect decreased content of NFκB transcription factor subunits, since Western blot analysis indicated no statistically significant difference in the amount of p50 and p65 in control *vs*. Grx1 knockdown cells (data not shown).

Inhibition of NFκB-dependent transcription is sufficient to sensitize H9c2 cells to oxidant-induced apoptosis

To determine whether diminution of NFκB activity by a similar extent as seen in Grx1-deficient cells is sufficient to increase apoptotic susceptibility in H9c2 cells, wild-type H9c2 cells were treated with the IKK inhibitor BMS 345541 (5). Both NFκB activity and apoptotic susceptibility were assessed following inhibitor treatment. BMS treatment resulted in dose-dependent diminution in NFκB activity (Fig. 6A), as well as increased susceptibility to apoptosis compared to untreated cells, in the presence and absence of H_2O_2 (Fig. 6B). Importantly, the concentration of BMS at which NFκB-dependent transcription was decreased by ~30% (*i.e.*, the amount of diminution observed in Grx1-deficient cells) was sufficient to increase apoptotic susceptibility, suggesting that ~30% inhibition of the NFκB pathway could contribute to the increased apoptotic susceptibility of Grx1-deficient cells.

mRNA and protein content of Bcl-2 and Bcl-xL are decreased in Grx1-deficient cells

Anti-apoptotic NFκB target genes Bcl-2 and Bcl-xL promote cellular survival in many cell types, including cardiomyocytes (reviewed in Ref. 12). In transgenic mouse models, Bcl-2 and Bcl-xL protect cardiomyocytes from apoptosis and improve cardiac function, particularly in the contexts of ischemia-reperfusion injury and heart failure (*e.g.*, [4, 15, 16, 31]). Conversely, decreases in Bcl-2 and/or Bcl-xL are associated with increased cardiomyocyte apoptosis in experimental models of ischemia (3, 22). We hypothesized that the increased apoptotic susceptibility in Grx1-deficient cells was due to decreased NFκB-dependent transcription of Bcl-2 and/or Bcl-xL. Indeed, real-time PCR analysis indicated that relative quantities of Bcl-2 and Bcl-xL mRNA were substantially decreased in Grx1-deficient cells (Fig. 7). Western blot analysis confirmed that contents of the Bcl-2 and Bcl-xL proteins were

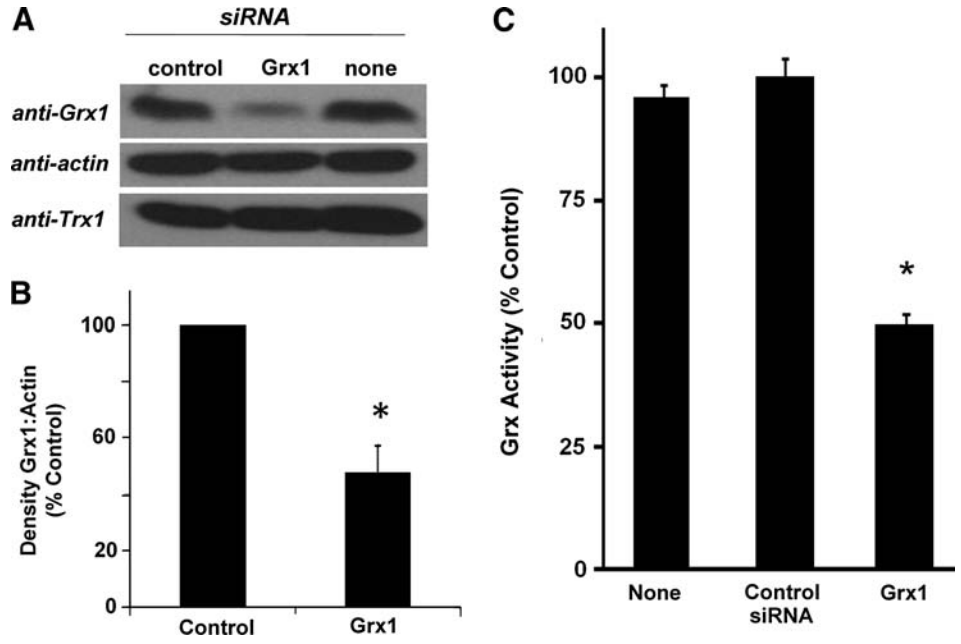

FIG. 3. Content of Grx1, but not Trx1, and total Grx activity are decreased *via* transfection of Grx1-targeted siRNA into H9c2 cells. (**A**) Representative Western blot showing Grx1 and Trx1 contents in H9c2 cells transfected with Grx1-targeted siRNA compared to control (scrambled) siRNA and nontransfected cells (none) (see *Materials and Methods*). (**B**) Quantification of densitometric analysis (relative density: Grx1/actin) of six Western blots of H9c2 cells transfected with control or Grx1-targeted siRNA (Grx1 content in Grx1 knockdown cells is decreased [*i.e.*, $52 \pm 9\%$ (mean $\pm$ SEM) decreased compared to control cells (100%)], $^{*}p < 0.03$. (**C**) Total Grx activity in H9c2 cells transfected with control or Grx1-targeted siRNA. Cell lysates were added to assay mix containing Na/K buffer, pH 7.5 (0.1 *M*), GSH (0.5 m*M* final), NADPH (0.2 m*M* final), and GR (1 U/mL, final). Cysteine-glutathione mixed disulfide (CSSG, 0.1 m*M* final) was added to initiate the reaction, and the rate of NADPH oxidation (reflecting the amount of GSSG formed, see *Materials and Methods*) was measured by monitoring A_{340} for 5 min at 30°C. Grx activity (3.09 ± 0.12 nmol NADPH oxidized/min/mg total protein in control cells; 2.93 ± 0.11 nmol/min/mg in nontransfected cells; and 1.52 ± 0.08 nmol/min/mg in Grx1 knockdown cells) was normalized to the value determined in control cells. Data represent mean $\pm$ SEM ($n = 4$, $p < 0.001$). *Analogous decreases in Grx1 content and total Grx activity were observed when Grx1 was stably knocked down in H9c2 cells using shRNA (see text in Results section).*

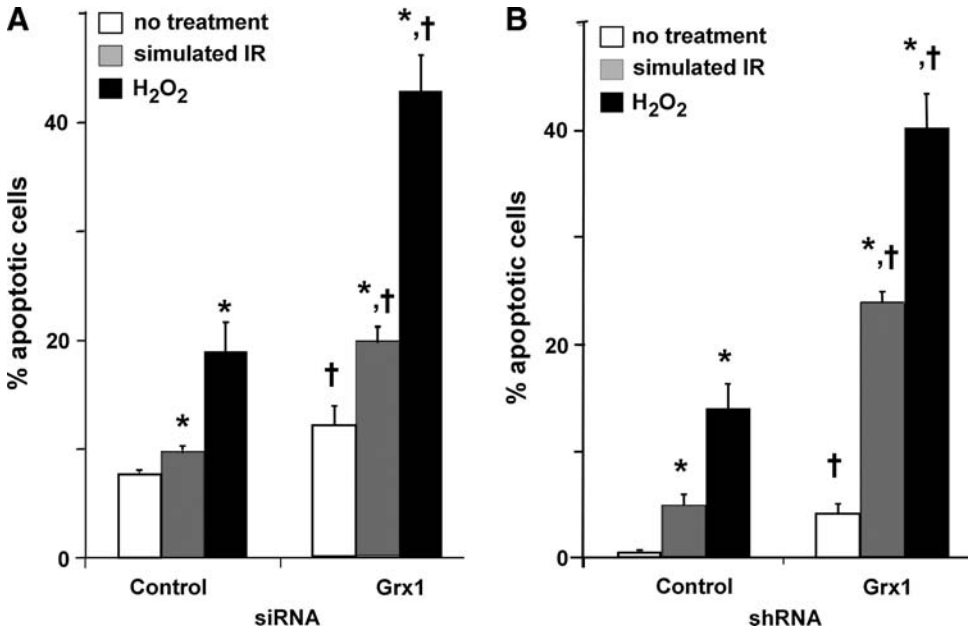

FIG. 4. Grx1 knockdown increases apoptotic susceptibility in H9c2 cells. H9c2 cells transfected with control or Grx1-targeted siRNA (see *Materials and Methods*) were subjected to H_2O_2 treatment (400 μM for 5 min, followed by 24 h recovery (13) or simulated ischemia/reperfusion (3 h substrate depletion, hypoxia, and acidosis, followed by 2 h recovery (21)), and apoptosis was assessed by Hoechst staining. (**A**) H9c2 cells in which Grx1 has been diminished by transient transfection with siRNA. (**B**) H9c2 cells in which Grx1 has been stably knocked-down using shRNA (see *Materials and Methods*). Data are represented as mean $\pm$ SEM. $^{*}p < 0.02$ compared to no treatment; $^{\dagger}p < 0.02$ compared to control siRNA or shRNA ($n = 5$–10). *Open bars*, no treatment; *shaded bars*, simulated IR; *closed bars*, H_2O_2.

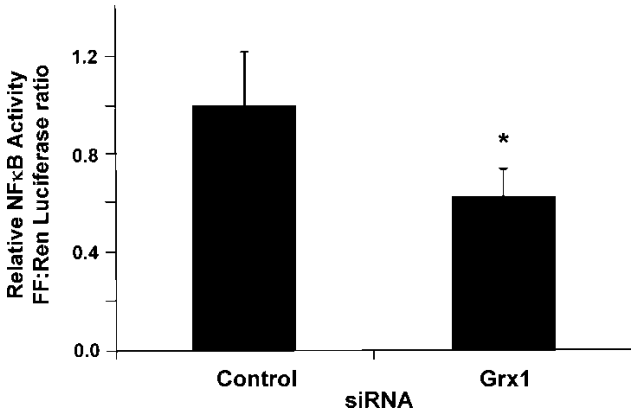

FIG. 5. Grx1-deficient cells exhibit decreased NFκB transcriptional activity. H9c2 cells were transfected with control or Grx1-targeted siRNA as described in *Materials and Methods*, then co-transfected with NFκB-Luciferase and Renilla plasmids. NFκB-dependent transcriptional activity was determined *via* a standard Dual-Luciferase assay. Renilla luciferase activity served as a transfection control, and data are represented as ratios of Firefly/Renilla activity, normalized to the mean ratio observed in control cells (mean ± SEM = 33.9 ± 7.4), *$p < 0.04$, $n = 4$.

also diminished substantially (~50%) with knockdown of Grx1 (Fig. 8).

Effect of decreased Bcl-2, Bcl-xL, or both on oxidant-induced apoptosis in H9c2 cells

To determine the relative contributions of decreased Bcl-2 and Bcl-xL in H9c2 cells, the proteins were knocked down individually or together (Figs. 9A–9D), and apoptotic susceptibility was assessed both at baseline and following H_2O_2 treatment (Figu. 9E). Knockdown of Bcl-2 *or* Bcl-xL in H9c2 cells increased apoptosis at baseline, each to a level comparable with that observed in Grx1 knockdown cells. In contrast, only knockdown of Bcl-xL increased *oxidant-induced* apoptosis in H9c2 cells, with the percentage of apoptotic cells closely matching that observed with Grx1 knockdown. Importantly, knockdown of Bcl-2 or Bcl-xL did not affect expression of the other protein (Fig. 9C). Simultaneous knockdown of Bcl-2 and Bcl-xL resulted in an apoptotic phenotype that was statistically indistinguishable from Bcl-xL knockdown alone.

NFκB activity in cardiomyocytes from adult and elderly F344 rats

Cytosolic extracts prepared from elderly (24–28 mo) F344 rat heart tissue exhibited decreased Grx1 content and total Grx activity compared to adult control samples (6–10 mo), and a similar diminution in Grx activity was observed in lysates of cardiomyocytes isolated from elderly *vs*. adult F344 rat hearts (see Fig.1). To determine whether NFκB activity is decreased also in elderly cardiomyocytes (as with Grx1 knockdown in H9c2 cells), NFκB-dependent transcription was measured in cardiomyocytes isolated from adult and elderly F344 rats. Indeed, cardiomyocytes from elderly F344 rats exhibited substantially lower NFκB-dependent transcriptional activity compared to adult controls (activity = 30 ± 9% of the adult control value, Fig. 10A), and there was a corresponding decrease in Bcl-xL content (Fig. 10B).

Discussion

The current study examined the role of glutaredoxin (Grx1) in modulation of apoptosis in cardiomyocytes, and identified a NFκB-dependent mechanism by which diminution of Grx1 may contribute to increased apoptotic susceptibility in the

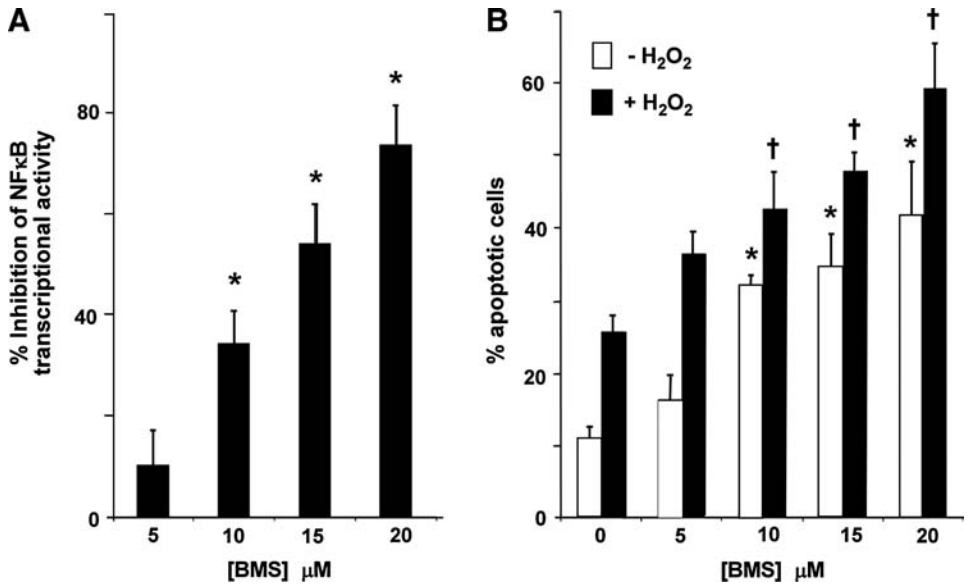

FIG. 6. Effect of IKK inhibitor BMS 345541 on NFκB activity and apoptotic susceptibility in wild-type H9c2 cells. (**A**) Dose-response of BMS 345541 on NFκB-dependent transcriptional activity. H9c2 cells were transfected with 5X NFκB-Firefly Luciferase plasmid for 8 h, treated with various concentrations of BMS 345541 for 15 h, and collected for determination of Luciferase activity. Percent inhibition of NFκB activity was calculated relative to activity in untreated cells (mean ± SEM = 1264 ± 99 RLU/mg). (**B**) Effect of BMS 345541 treatment on sensitivity of H9c2 cells to H_2O_2-induced apoptosis. H9c2 cells treated as described above were subjected to 400 μM H_2O_2 (or no H_2O_2) for 5 min., then incubated for 24 h and assayed for apoptosis by Hoechst staining. *Open bars* (□), no treatment; *closed bars* (■), H_2O_2. *$p < 0.02$ *vs*. no BMS treatment (no H_2O_2); †$p < 0.02$ *vs*. no BMS treatment (with H_2O_2), $n = 4$.

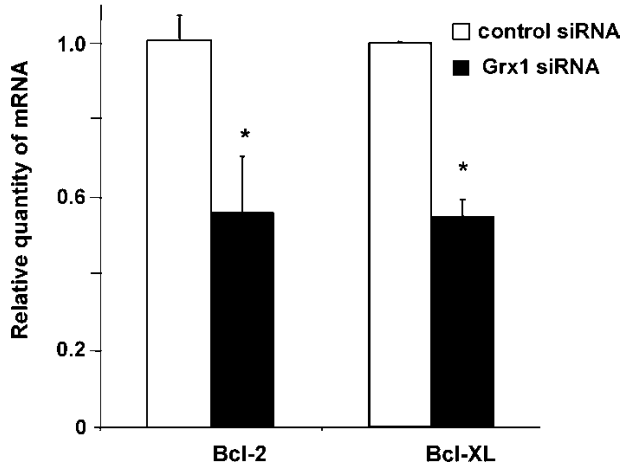

FIG. 7. Relative amounts of Bcl-2 and Bcl-xL mRNA in Grx1 knockdown cells normalized to amounts in control cells. Real-time PCR analysis was performed on mRNA isolated from control and Grx1 knockdown H9c2 cells as detailed in *Materials and Methods*. Data are expressed as ratios of the relative quantities of Bcl-2 and Bcl-xL mRNA measured in Grx1 knockdown cells compared to control cells. *Open bars* (□), control cells; *closed bars* (■), Grx1 knockdown cells. Each *n* represents at least duplicate determinations from a single Grx1 knockdown experiment. For Bcl-2, data represent mean ± SEM, $n = 4$; for Bcl-xL, data represent mean ± range of values for analysis of two samples. For each experiment, Grx1 knockdown was verified separately by Western blot analysis *(data consistent with Fig. 3)*, $^*p < 0.01$.

elderly. We found that Grx1 content and total Grx activity are decreased in heart tissue and in cardiomyocytes isolated from elderly Fischer 344 rats, a well-established animal model of aging, whereas other thiol-disulfide oxidoreductase enzymes were found to be little changed. Based on observations that many apoptotic mediators are subject to regulation by reversible glutathionylation (36, 39, 41), and that overexpression of Grx1 protects H9c2 cardiomyocytes from oxidant-induced apoptosis (32), we hypothesized that the age-related decrease in Grx1 contributes to the increased susceptibility to apoptosis already documented in cardiomyocytes from elderly animals (19, 26, 34). Therefore we knocked down Grx1 in H9c2 cells to a similar extent as in cardiomyocytes from elderly rats to assess the independent contribution of diminished Grx1 to apoptotic susceptibility.

Selective diminution of Grx1 indeed led to an increase in apoptotic cells at baseline, as well as following oxidative insults previously shown to trigger cardiomyocyte apoptosis (13, 21). It is noteworthy that both transient (siRNA) or stable (shRNA) knockdown of Grx1 led to analogous increases in oxidant-induced apoptotic susceptibility of the model cardiomyocytes, because the latter approach is more akin to the decrease in Grx1 in the cells from elderly animals. Transcriptional activity of NFκB, a transcription factor with anti-apoptotic effects in cardiomyocytes (2, 33), was concomitantly decreased in both Grx1 knockdown cells and in primary cardiomyocytes isolated from elderly F344 rats, likely accounting for the increased apoptotic susceptibility in Grx1-deficient cells. Support for this interpretation is provided by the observation that inhibition of NFκB-dependent transcription to the same extent as in Grx1 knockdown cells led to increased apoptosis both at baseline and following H_2O_2 treatment (Fig. 6).

mRNA and protein contents of the anti-apoptotic NFκB transcription products Bcl-2 and Bcl-xL were decreased by about 50% in Grx-deficient cells. Knockdown of Bcl-2 and/or Bcl-xL in H9c2 cells to a similar extent (*i.e.*, ~40%–60%) increased apoptosis at baseline, suggesting that diminution of these anti-apototic factors contributes to the increased apoptosis of resting Grx1-deficient cells. In remarkable contrast, knockdown of Bcl-2 alone had *no effect* on oxidant-induced apoptosis in H9c2 cells, whereas diminution of Bcl-xL alone (or in combination with Bcl-2 knockdown) increased oxidant-induced apoptosis to the same extent as observed in Grx1 knockdown cells, *fully accounting for the apoptotic phenotype of these cells*. Taken together, these observations suggest a mechanism for the increased apoptotic susceptibility of

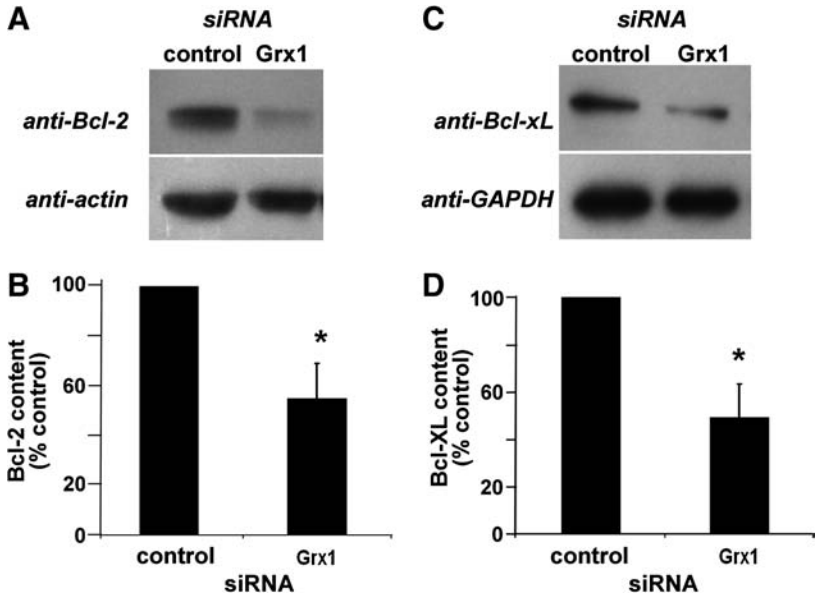

FIG. 8. Contents of Bcl-2 and Bcl-xL proteins are decreased in Grx1-deficient H9c2 cells. Contents of Bcl-2 and Bcl-xL, both anti-apoptotic NFκB target genes, were compared in control and Grx1 knockdown cells by Western blot analysis. (**A**) Representative Western blot showing diminished Bcl-2 in Grx1 knockdown cells. (**B**) Quantification of six Western blots showing Bcl-2 content (normalized to actin, 45 ± 14% decrease in Grx1 knockdown cells), $^*p < 0.03$ *vs.* control siRNA. (**C**) Representative Western blot showing diminished Bcl-xL in Grx1 knockdown cells. (**D**) Quantification of four Western blots showing Bcl-xL content (normalized to GAPDH), 50 ± 14% decrease in Grx1 knockdown cells, $^*p < 0.02$ *vs.* control siRNA.

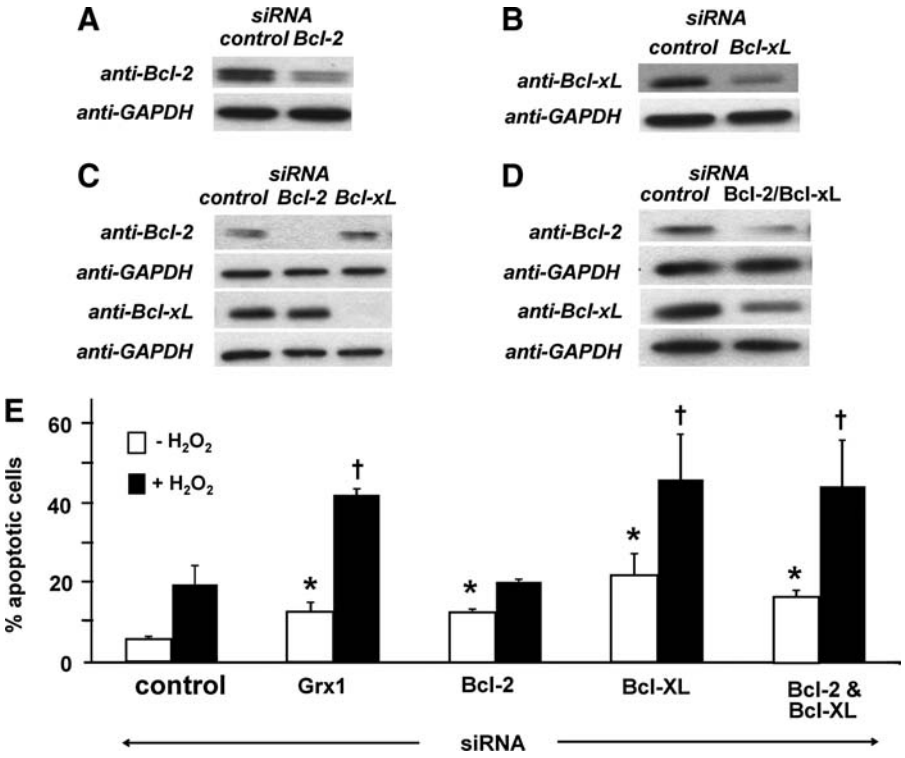

FIG. 9. Effect of Bcl-2 and Bcl-xL knockdown on apoptotic susceptibility in H9c2 cells. (**A**) Content of Bcl-2 was diminished *via* transfection with targeted siRNA as described in *Materials and Methods*. Representative Western blot analysis of Bcl-2 content in control and Bcl-2 knockdown H9c2 cells (knockdown = 63 ± 4%, $n = 3$). (**B**) Content of Bcl-xL was diminished *via* transfection with targeted siRNA as described in *Materials and Methods*. Representative Western blot analysis of Bcl-xL in control and Bcl-xL knockdown H9c2 cells (knockdown = 45 ± 7%, $n = 6$). (**C**) Complete knockdown of Bcl-2 or Bcl-xL does not affect expression of the other protein. H9c2 cells were treated with sufficient concentrations of Bcl-2- or Bcl-xL-targeted siRNA *to reduce the target protein to undetectable levels*, and content of each protein was determined by Western blotting. Bcl-2 content in Bcl-xL knockdown cells were 116 ± 13% (mean ± SEM) of the value in control cells ($n = 9$). Bcl-xL content in Bcl-2 knockdown cells was 97 ± 10% (mean ± SEM) of the value in control cells ($n = 4$). (**D**) Bcl-2 and Bcl-xL content were both diminished *via* transfection with targeted siRNA. Representative Western blot showing ~40% simultaneous knockdown of both Bcl-2 and Bcl-xL in H9c2 cells (Bcl-2 knockdown: 45 ± 3%; Bcl-xL knockdown: 37 ± 6%, $n = 6$). (**E**) Apoptosis in control, Bcl-2 knockdown, Bcl-xL knockdown, and Bcl-2/Bcl-xL double knockdown cells ± H_2O_2 treatment (400 μM for 5 min, followed by 24 h recovery, see *Materials and Methods*). *Open bars* (□), no treatment; *closed bars* (■), H_2O_2. Data represent mean % apoptotic cells ± SEM ($n = 3$–10). *$p < 0.05$ *vs.* control siRNA (without H_2O_2); †$p < 0.05$ *vs.* control siRNA (with H_2O_2).

aging cardiomyocytes in which diminished Grx1 leads to decreased NFκB activity, resulting in decreased content of anti-apoptotic proteins and a lower threshold for commitment to apoptosis.

Control of apoptotic susceptibility by Grx1 via regulation of NFκB

Grx1 has been implicated in the regulation of apoptosis *via* modulation of the glutathionylation status of apoptotic mediators, including NFκB (30). S-glutathionylation is inhibitory towards many NFκB signaling intermediates, (*e.g.*, IKK, p50, p65, 20S proteasome, and ubiquitin-activating and -carrier proteins [reviewed in Ref. 30]) and increased expression of Grx1, the primary intracellular *deglutathionylating* enzyme, is correlated with increased NFκB transcriptional activity (14, 41, 45). Thus, in most cases, Grx1 activity is expected to support NFκB activity, likely *via deglutathionylation* of one or more mediators in the NFκB signaling pathway. A notable exception is in hypoxic pancreatic cancer cells, where Grx1 enhances the *glutathionylation* of p65, leading to decreased DNA binding and diminished NFκB transcriptional activity (39).

We observed *decreased* NFκB activity in Grx1 knockdown H9c2 cells as well as in Grx1-deficient (elderly) primary cardiomyocytes. Thus, the likely mechanism of NFκB regulation by Grx1 in these cardiomyocytes is direct *deglutathionylation* (activation) of one or more components of the NFκB axis, so that diminution of Grx1 activity leads to increased glutathionylation and deactivation of one or more control points in the pathway. The specific site(s) of regulation of the NFκB pathway in the Grx1 knockdown H9c2 cells (and in the aging heart) is not known, and identifying these sites represents a natural direction for future studies. Besides the signaling intermediates described above, other possibilities include upstream activators (*e.g.*, Akt, Ras) or inhibitors (*e.g.*, PTEN) (reviewed in Ref. 30). Other investigators have presented evidence for activation of Akt activity in H9c2 cells and heart tissue by Grx1 (27, 32), but the relationship between those studies that involved overexpression of Grx1 and the effects of Grx1 diminution in aging remains to be elucidated.

To our knowledge, this is the first report of diminished NFκB activity in the aging heart, documented in cardiomyocytes from adult and elderly rats. NFκB activity was reported to be *increased* with aging in cardiac tissue from Sprague–Dawley rats (11); however, this conclusion appears to be based on increased content of p65 in the nucleus, which is necessary but not sufficient for NFκB transcriptional activity. Age-associated changes (increases or decreases) in NFκB activity have been reported in various other contexts also (35, 38); apparently reflecting tissue- and organism-specific differences in regulation.

Studies of thiol–disulfide oxidoreductase systems with aging also yield a complex picture, reflecting tissue-, organism- and sex-specific differences. We found Grx1 content and

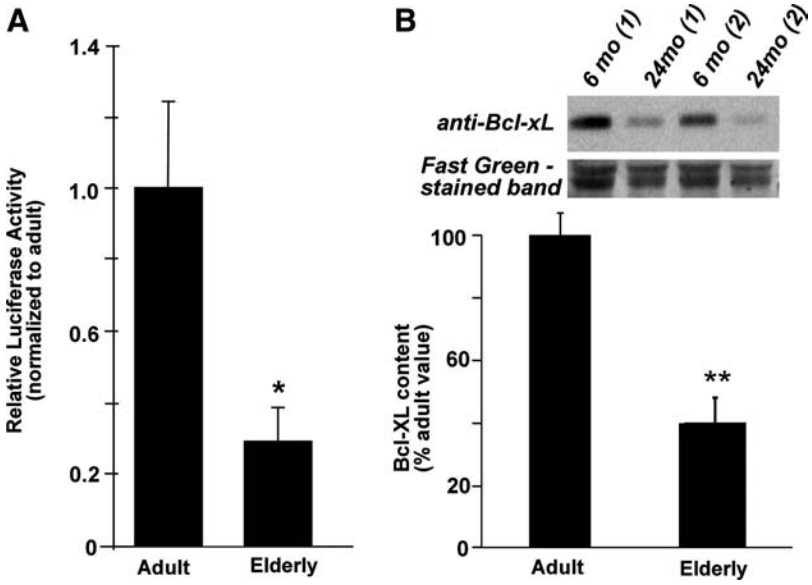

FIG. 10. (A) NFκB-dependent transcriptional activity in cardiomyocytes isolated from adult and elderly F344 rat hearts. Cardiomyocytes were isolated from adult and elderly F344 rat hearts *via* collagenase digestion of connective tissue as described in *Materials and Methods*. Immediately following isolation, cardiomyocytes were co-infected with an adenovirus encoding Renilla luciferase (MOI ~20), and an adenovirus encoding the NFκB promoter, followed by firefly Luciferase (MOI ~100). Cells were plated, cultured for 24 h, and collected for analysis of luciferase activities. Ratios of firefly luciferase:Renilla luciferase activities were determined for each preparation of cardiomyocytes, then normalized to the value for adult animals (mean ± SEM = 13.1 ± 3.3). For elderly rats, cardiomyocytes from two animals were pooled for each experiment (*i.e.*, each *n* number). For adult rats, $n = 7$; for elderly rats, $n = 9$; *$p < 0.02$. (**B**) Bcl-xL content in cardiomyocytes isolated from adult and elderly F344 rat hearts. Immediately following isolation, cardiomyocytes were lysed in RIPA lysis buffer (150 m*M* NaCl, 1 m*M* EGTA, 1% sodium deoxycholate, 1% Triton X-100, 50 m*M* Tris-Cl, pH 7.4) supplemented with a cocktail of protease inhibitors as described in *Materials and Methods*. Cardiomyocyte lysates were analyzed for total protein and for Bcl-xL (see *Methods*) using Western blotting (40 μg of protein/lane). The same blot was stained with Fast green FCF dye (Sigma) to monitor equal loading, and relative Bcl-xL protein levels were calculated by densitometric analysis. Densitometric ratios (Bcl-xL/Fast Green-stained band) were determined for samples of lysed cardiomyocytes from adult and elderly rats. The ratio for adult cardiomyocytes (mean ± SEM = 2.8 ± 0.21) was set to 100%. Data are presented as normalized means ± SEM for at least three ($n = 3$) independent preparations of cardiomyocytes from adult and elderly rats; **$p < 0.005$.

activity decreased in cytosol from elderly F344 rat hearts, while Trx, TR, and GR were not changed significantly. Suh *et al.* (50) reported a decrease in Grx activity in interfibrillar but not subsarcolemmal mitochondria from F344 rat hearts. In F344 rat liver, aging was reported to have no effect on Grx, TR, or protein disulfide isomerase activities, while GR activity was increased in females, but not in males (42). In Wistar rat kidney, TR activity was *decreased* by 50% with aging, while GR activity remained constant (44). Finally, Trx content was reported to increase somewhat with aging in mice, but net Trx activity, and its association with ASK1, were diminished due to nitration of Trx tyrosine residues (56).

Significance of Bcl-2 and Bcl-xL diminution in susceptibility to cardiomyocyte apoptosis

Our studies implicate decreases in the anti-apoptotic NFκB target genes Bcl-2 and Bcl-xL in the increased apoptotic susceptibility of Grx1 knockdown cells at rest, and suggest a special role for Bcl-xL in protection of cardiomyocytes from *oxidant-induced* apoptosis. The distinct effects of knocking down Bcl-2 and/or Bcl-xL in H9c2 cells suggest separate, but overlapping, cytoprotective roles for these two proteins in cardiomyocytes, consistent with recent reports documenting both shared and distinct anti-apoptotic mechanisms (*e.g.*, (12, 43, 54). The increased sensitivity of H9c2 cells to Bcl-xL knockdown compared to Bcl-2 knockdown is consistent with the findings of Feibig *et al.* (9), who observed that Bcl-xL is a more potent anti-apoptotic molecule than Bcl-2 in T-cells subjected to oxidative stress by Doxorubicin treatment.

Conclusion

The potential of the thiol–disulfide oxidoreductase enzymes (thioredoxin and glutaredoxin systems) in defense against oxidative stress with aging has been noted previously (51). However, there has been little direct information about the Grx and Trx systems in this regard. Sohal's group provided evidence for a protective role of glutaredoxin and GSH in the aging process, displaying higher contents in longer-lived houseflies (47). By analogy it is reasonable to expect changes in thiol–disulfide oxidoreductase activity to contribute to the complications of aging in mammals also, and the current study supports this interpretation. Thus, we present evidence that diminution of Grx1 predisposes cardiomyocytes to apoptosis by decreasing NFκB activity, resulting in downregulation of its anti-apoptotic target genes Bcl-2 and Bcl-xL. Targeted knockdown studies with H9c2 cells suggest that Bcl-xL plays a more important role in protection of cardiomyocytes from oxidant-induced apoptosis. Taken together with observations that Grx1 and NFκB activities and Bcl-xL content are diminished in the hearts of elderly F344 rats, these data provide a mechanistic explanation for why cardiomyocytes in the hearts of the elderly exhibit increased susceptibility to apoptosis, and further implicate Bcl-xL as an important anti-apoptotic molecule in the heart.

Acknowledgments

These studies were presented in part at the American Heart Association Scientific Sessions, Orlando, 2007 (Abstract #1328). The authors gratefully acknowledge Sarah Stewart for

technical assistance in the isolation of primary cardiomyocytes, as well as Drs. David Roth and Hemal Patel (University of California, San Diego, Department of Anesthesiology) for assistance with optimization of the isolation protocol. We thank Dr. Margaret Chandler (CWRU Dept. of Physiology and Biophysics) for overseeing the purchase and maintenance of animals before use in experiments. Jason Molitoris (Dr. Clark Distelhorst's laboratory, CWRU Dept. of Pharmacology) assisted with preparation of mRNA for real-time PCR, and Dr. Martina Veigl and Vaibav Pathak (CWRU Gene Expression and Genotyping Core Facility) performed real-time PCR analysis. Tyler Murphy (CWRU Dept. of Pharmacology) conducted Western blot analysis of Trx1 content, and Elizabeth Sabens captured images of isolated cardiomyocytes. We thank Dr. Clark Distelhorst (CWRU Dept. of Pharmacology) for reviewing the manuscript prior to submission. This work was supported by the following NIH Grants: R01 AG024413 (JJM), P01 AG15885 (JJM, EJL, CLH), F30 AG029687A (MMG), T32 GM008803 (MMG), T32 GM07250 (MMG), and T32 EY07157 (MDS), and a VA Merit Review grant (JJM).

Author Disclosure Statement

No competing financial interests exist.

References

1. Arner ES, Zhong L, and Holmgren A. Preparation and assay of mammalian thioredoxin and thioredoxin reductase. *Methods Enzymol* 300: 226–239, 1999.
2. Bergmann MW, Loser P, Dietz R, and von HR. Effect of NF-kappa B Inhibition on TNF-alpha-induced apoptosis and downstream pathways in cardiomyocytes. *J Mol Cell Cardiol* 33: 1223–1232, 2001.
3. Bonavita F, Stefanelli C, Giordano E, Columbaro M, Facchini A, Bonafe F, Caldarera CM, and Guarnieri C. H9c2 cardiac myoblasts undergo apoptosis in a model of ischemia consisting of serum deprivation and hypoxia: Inhibition by PMA. *FEBS Lett* 536: 85–91, 2003.
4. Brocheriou V, Hagege AA, Oubenaissa A, Lambert M, Mallet VO, Duriez M, Wassef M, Kahn A, Menasche P, and Gilgenkrantz H. Cardiac functional improvement by a human Bcl-2 transgene in a mouse model of ischemia/reperfusion injury. *J Gene Med* 2: 326–333, 2000.
5. Burke JR, Pattoli MA, Gregor KR, Brassil PJ, MacMaster JF, McIntyre KW, Yang X, Iotzova VS, Clarke W, Strand J, Qiu Y, and Zusi FC. BMS-345541 is a highly selective inhibitor of I kappa B kinase that binds at an allosteric site of the enzyme and blocks NF-kappa B-dependent transcription in mice. *J Biol Chem* 278: 1450–1456, 2003.
6. Chen YR, Chen CL, Pfeiffer DR, and Zweier JL. Mitochondrial complex II in the post-ischemic heart: oxidative injury and the role of protein S-glutathionylation. *J Biol Chem* 282: 32640–32654, 2007.
7. Chrestensen CA, Starke DW, and Mieyal JJ. Acute cadmium exposure inactivates thioltransferase (Glutaredoxin), inhibits intracellular reduction of protein-glutathionyl-mixed disulfides, and initiates apoptosis. *J Biol Chem* 275: 26556–26565, 2000.
8. Eaton P, Wright N, Hearse DJ, and Shattock MJ. Glyceraldehyde phosphate dehydrogenase oxidation during cardiac ischemia and reperfusion. *J Mol Cell Cardiol* 34: 1549–1560, 2002.
9. Fiebig AA, Zhu W, Hollerbach C, Leber B, and Andrews DW. Bcl-XL is qualitatively different from and ten times more effective than Bcl-2 when expressed in a breast cancer cell line. *BMC Cancer* 6: 213, 2006.
10. Gallogly MM, Starke DW, and Mieyal JJ. Mechanistic and kinetic details of thiol-disulfide exchange by glutaredoxins and potential mechanisms of regulation. *Antioxid Redox Signal* 11: 1059–1081, 2009.
11. Gao ZQ, Yang C, Wang YY, Wang P, Chen HL, Zhang XD, Liu R, Li WL, Qin XJ, Liang X, and Hai CX. RAGE upregulation and nuclear factor-kappaB activation associated with ageing rat cardiomyocyte dysfunction. *Gen Physiol Biophys* 27: 152–158, 2008.
12. Gustafsson AB and Gottlieb RA. Bcl-2 family members and apoptosis, taken to heart. *Am J Physiol Cell Physiol* 292: C45–C51, 2007.
13. Han H, Long H, Wang H, Wang J, Zhang Y, and Wang Z. Progressive apoptotic cell death triggered by transient oxidative insult in H9c2 rat ventricular cells: A novel pattern of apoptosis and the mechanisms. *Am J Physiol Heart Circ Physiol* 286: H2169–H2182, 2004.
14. Hirota K, Matsui M, Murata M, Takashima Y, Cheng FS, Itoh T, Fukuda K, and Yodoi J. Nucleoredoxin, glutaredoxin, and thioredoxin differentially regulate NF-kappaB, AP-1, and CREB activation in HEK293 cells. *Biochem Biophys Res Commun* 274: 177–182, 2000.
15. Huang J, Ito Y, Morikawa M, Uchida H, Kobune M, Sasaki K, Abe T, and Hamada H. Bcl-xL gene transfer protects the heart against ischemia/reperfusion injury. *Biochem Biophys Res Commun* 311: 64–70, 2003.
16. Imahashi K, Schneider MD, Steenbergen C, and Murphy E. Transgenic expression of Bcl-2 modulates energy metabolism, prevents cytosolic acidification during ischemia, and reduces ischemia/reperfusion injury. *Circ Res* 95: 734–741, 2004.
17. Jao SC, English Ospina SM, Berdis AJ, Starke DW, Post CB, and Mieyal JJ. Computational and mutational analysis of human glutaredoxin (thioltransferase): probing the molecular basis of the low pKa of cysteine 22 and its role in catalysis. *Biochemistry* 45: 4785–4796, 2006.
18. Jones WK, Brown M, Wilhide M, He S, and Ren X. NF-kappaB in cardiovascular disease: Diverse and specific effects of a "general" transcription factor? *Cardiovasc Toxicol* 5: 183–202, 2005.
19. Kajstura J, Cheng W, Sarangarajan R, Li P, Li B, Nitahara JA, Chapnick S, Reiss K, Olivetti G, and Anversa P. Necrotic and apoptotic myocyte cell death in the aging heart of Fischer 344 rats. *Am J Physiol* 271: H1215–H1228, 1996.
20. Kalogeropoulos A, Georgiopoulou V, Kritchevsky SB, Psaty BM, Smith NL, Newman AB, Rodondi N, Satterfield S, Bauer DC, Bibbins–Domingo K, Smith AL, Wilson PW, Vasan RS, Harris TB, and Butler J. Epidemiology of incident heart failure in a contemporary elderly cohort: The health, aging, and body composition study. *Arch Intern Med* 169: 708–715, 2009.
21. Kim JS, Jin Y, and Lemasters JJ. Reactive oxygen species, but not Ca2 + overloading, trigger pH- and mitochondrial permeability transition-dependent death of adult rat myocytes after ischemia-reperfusion. *Am J Physiol Heart Circ Physiol* 290: H2024–H2034, 2006.
22. Lazou A, Iliodromitis EK, Cieslak D, Voskarides K, Mousikos S, Bofilis E, and Kremastinos DT. Ischemic but not mechanical preconditioning attenuates ischemia/reperfusion induced myocardial apoptosis in anaesthetized rabbits: The role of Bcl-2 family proteins and ERK1/2. *Apoptosis* 11: 2195–2204, 2006.

23. Lee Y and Gustafsson AB. Role of apoptosis in cardiovascular disease. *Apoptosis* 14: 536–548, 2009.
24. Lesnefsky EJ, Lundergan CF, Hodgson JM, Nair R, Reiner JS, Greenhouse SW, Califf RM, and Ross AM. Increased left ventricular dysfunction in elderly patients despite successful thrombolysis: The GUSTO-I angiographic experience. *J Am Coll Cardiol* 28: 331–337, 1996.
25. Lieber SC, Aubry N, Pain J, Diaz G, Kim SJ, and Vatner SF. Aging increases stiffness of cardiac myocytes measured by atomic force microscopy nanoindentation. *Am J Physiol Heart Circ Physiol* 287: H645–H651, 2004.
26. Liu P, Xu B, Cavalieri TA, and Hock CE. Age-related difference in myocardial function and inflammation in a rat model of myocardial ischemia-reperfusion. *Cardiovasc Res* 56: 443–453, 2002.
27. Malik G, Nagy N, Ho YS, Maulik N, and Das DK. Role of glutaredoxin-1 in cardioprotection: An insight with Glrx1 transgenic and knockout animals. *J Mol Cell Cardiol* 44: 261–269, 2008.
28. Mani K. Programmed cell death in cardiac myocytes: Strategies to maximize post-ischemic salvage. *Heart Fail Rev* 13: 193–209, 2008.
29. Maulik N, Engelman RM, Rousou JA, Flack JE, III, Deaton D, and Das DK. Ischemic preconditioning reduces apoptosis by upregulating anti-death gene Bcl-2. *Circulation* 100: II369–II375, 1999.
30. Mieyal JJ, Gallogly MM, Qanungo S, Sabens EA, and Shelton MD. Molecular mechanisms and clinical implications of reversible protein S-glutathionylation. *Antioxid Redox Signal* 10: 1941–1988, 2008.
31. Moorjani N, Catarino P, Trabzuni D, Saleh S, Moorji A, Dzimiri N, Al–Mohanna F, Westaby S, and Ahmad M. Upregulation of Bcl-2 proteins during the transition to pressure overload-induced heart failure. *Int J Cardiol* 116: 27–33, 2007.
32. Murata H, Ihara Y, Nakamura H, Yodoi J, Sumikawa K, and Kondo T. Glutaredoxin exerts an antiapoptotic effect by regulating the redox state of Akt. *J Biol Chem* 278: 50226–50233, 2003.
33. Mustapha S, Kirshner A, De MD, and Kirshenbaum LA. A direct requirement of nuclear factor-kappa B for suppression of apoptosis in ventricular myocytes. *Am J Physiol Heart Circ Physiol* 279: H939–H945, 2000.
34. Nitahara JA, Cheng W, Liu Y, Li B, Leri A, Li P, Mogul D, Gambert SR, Kajstura J, and Anversa P. Intracellular calcium, DNase activity and myocyte apoptosis in aging Fischer 344 rats. *J Mol Cell Cardiol* 30: 519–535, 1998.
35. Okaya T, Blanchard J, Schuster R, Kuboki S, Husted T, Caldwell CC, Zingarelli B, Wong H, Solomkin JS, and Lentsch AB. Age-dependent responses to hepatic ischemia/reperfusion injury. *Shock* 24: 421–427, 2005.
36. Pan S and Berk BC. Glutathiolation regulates tumor necrosis factor-alpha-induced caspase-3 cleavage and apoptosis: Key role for glutaredoxin in the death pathway. *Circ Res* 100: 213–219, 2007.
37. Patel HH, Head BP, Petersen HN, Niesman IR, Huang D, Gross GJ, Insel PA, and Roth DM. Protection of adult rat cardiac myocytes from ischemic cell death: Role of caveolar microdomains and delta-opioid receptors. *Am J Physiol Heart Circ Physiol* 291: H344–H350, 2006.
38. Patel JR and Brewer GJ. Age-related differences in NFkappaB translocation and Bcl-2/Bax ratio caused by TNFalpha and Abeta42 promote survival in middle-age neurons and death in old neurons. *Exp Neurol* 213: 93–100, 2008.
39. Qanungo S, Starke DW, Pai HV, Mieyal JJ, and Nieminen AL. Glutathione supplementation potentiates hypoxic apoptosis by S-glutathionylation of p65-NFkappaB. *J Biol Chem* 282: 18427–18436, 2007.
40. Rebrin I and Sohal RS. Pro-oxidant shift in glutathione redox state during aging. *Adv Drug Deliv Rev* 60: 1545–1552, 2008.
41. Reynaert NL, van der Vliet A, Guala AS, McGovern T, Hristova M, Pantano C, Heintz NH, Heim J, Ho YS, Matthews DE, Wouters EF, and Janssen–Heininger YM. Dynamic redox control of NF-kappaB through glutaredoxin-regulated S-glutathionylation of inhibitory kappaB kinase beta. *Proc Natl Acad Sci USA* 103: 13086–13091, 2006.
42. Rikans LE and Hornbrook KR. Thiol–disulfide exchange systems in the liver of aging Fischer 344 rats. *Gerontology* 44: 72–77, 1998.
43. Rong Y and Distelhorst CW. Bcl-2 protein family members: Versatile regulators of calcium signaling in cell survival and apoptosis. *Annu Rev Physiol* 70: 73–91, 2008.
44. Santa MC and Machado A. Age and sex related differences in some rat renal NADPH-consuming detoxification enzymes. *Arch Gerontol Geriatr* 5: 235–247, 1986.
45. Shelton MD, Kern TS, and Mieyal JJ. Glutaredoxin regulates nuclear factor kappa-B and intercellular adhesion molecule in Muller cells: Model of diabetic retinopathy. *J Biol Chem* 282: 12467–12474, 2007.
46. Shelton MD and Mieyal JJ. Regulation by reversible S-glutathionylation: Molecular targets implicated in inflammatory diseases. *Mol Cells* 25: 332–346, 2008.
47. Sohal RS, Farmer KJ, and Allen RG. Correlates of longevity in two strains of the housefly, *Musca domestica. Mech Ageing Dev* 40: 171–179, 1987.
48. Song JJ, Rhee JG, Suntharalingam M, Walsh SA, Spitz DR, and Lee YJ. Role of glutaredoxin in metabolic oxidative stress. Glutaredoxin as a sensor of oxidative stress mediated by H2O2. *J Biol Chem* 277: 46566–46575, 2002.
49. Starke DW, Chen Y, Bapna CP, Lesnefsky EJ, and Mieyal JJ. Sensitivity of protein sulfhydryl repair enzymes to oxidative stress. *Free Radic Biol Med* 23: 373–384, 1997.
50. Suh JH, Heath SH, and Hagen TM. Two subpopulations of mitochondria in the aging rat heart display heterogenous levels of oxidative stress. *Free Radic Biol Med* 35: 1064–1072, 2003.
51. Tanaka T, Nakamura H, Nishiyama A, Hosoi F, Masutani H, Wada H, and Yodoi J. Redox regulation by thioredoxin superfamily; Protection against oxidative stress and aging. *Free Radic Res* 33: 851–855, 2000.
52. Tani M, Suganuma Y, Hasegawa H, Shinmura K, Ebihara Y, Hayashi Y, Guo X, and Takayama M. Decrease in ischemic tolerance with aging in isolated perfused Fischer 344 rat hearts: Relation to increases in intracellular Na + after ischemia. *J Mol Cell Cardiol* 29: 3081–3089, 1997.
53. Wang J, Boja ES, Tan W, Tekle E, Fales HM, English S, Mieyal JJ, and Chock PB. Reversible glutathionylation regulates actin polymerization in A431 cells. *J Biol Chem* 276: 47763–47766, 2001.
54. Wang X, Zhang J, Kim HP, Wang Y, Choi AM, and Ryter SW. Bcl-XL disrupts death-inducing signal complex formation in plasma membrane induced by hypoxia/reoxygenation. *FASEB J* 18: 1826–1833, 2004.
55. Willems L, Zatta A, Holmgren K, Ashton KJ, and Headrick JP. Age-related changes in ischemic tolerance in male and female mouse hearts. *J Mol Cell Cardiol* 38: 245–256, 2005.
56. Zhang H, Tao L, Jiao X, Gao E, Lopez BL, Christopher TA, Koch W, and Ma XL. Nitrative thioredoxin inactivation as a

cause of enhanced myocardial ischemia/reperfusion injury in the aging heart. *Free Radic Biol Med* 43: 39–47, 2007.
57. Zidar N, Jera J, Maja J, and Dusan S. Caspases in myocardial infarction. *Adv Clin Chem* 44: 1–33, 2007.

Address correspondence to:
John J. Mieyal
Department of Pharmacology
Case Western Reserve University School of Medicine
2109 Adelbert Road
Cleveland, OH 44106-4965

E-mail: jjm5@cwru.edu

Date of first submission to ARS Central, July 24, 2009; date of final revised submission, November 17, 2009; date of acceptance, November 17, 2009.

Abbreviations Used

6-mo = 6 month-old
24-mo = 24 month-old
Akt = protein kinase B
ASK1 = apoptosis signal-regulating kinase 1
BMS 345541 = (4(2-aminoethyl)amino-1,8-dimethylimidazo-(1,2-a)quinoxaline)
BSA = bovine serum albumin
DAPI = 4′,6-diamidino-2-phenylindole
DMEM = Dulbecco's modified Eagle medium
DTT = dithiothreitol
EDTA = ethylenediaminetetraacetic acid
F344 = Fischer 344
FBS = fetal bovine serum
GAPDH = glyceraldehyde 3-phosphate dehydrogenase
GR = glutathione disulfide reductase
Grx = glutaredoxin
GSH = glutathione
GSSG = glutathione disulfide
IκB = inhibitor of κB
IR = ischemia-reperfusion
MI = myocardial infarction
MOI = multiplicity of infection
NFκB = nuclear factor κB
PVDF = polyvinylidene difluoride
RLU = relative light units
SDS = sodium dodecyl sulfate
SEM = standard error of the mean
sIR = simulated ischemia-reperfusion
siRNA = small interfering RNA
TNF = tumor necrosis factor
TR = thioredoxin reductase
Trx = thioredoxin